KSCE Journal of Civil Engineering (2019) 23(1):367-375

DOI 10.1007/s12205-018-1093-4

Structural Engineering

pISSN 1226-7988, eISSN 1976-3808
www.springer.com/12205

TECHNICAL NOTE

Evaluation of Equivalent Bending Stiffness by Simplified Theoretical Solution for an FRP–aluminum Deck–truss Structure

Dongdong Zhang*, Feng Li, Fei Shao***, and Chengfei Fan******

Received May 31, 2018/Revised July 16, 2018/Accepted July 17, 2018/Published Online December 17, 2018

Abstract

A hybrid Fiber-Reinforced Polymer (FRP)–aluminum spatial deck–truss structure that incorporates an innovative structural form and advanced extrusion-type FRP profiles has the advantages of a lightweight, high-bearing capacity, and faster installation. In this study, a design-oriented investigation was conducted with a simplified theoretical solution to conveniently evaluate the equivalent bending stiffness of the above-mentioned unique structure. The simplified theoretical solution was derived using the equivalent continuum beam method based on the homogenization concept and shearing equivalence principle. The theoretical prediction enabled a direct format and simple calculation process convenient for engineers in terms of the calculation and design. The theoretical solution was experimentally and numerically calibrated to ensure that the formulae have the satisfactory accuracy. The accuracy of the predicted bending stiffness exceeded 90%. The derivation procedures and formulae further indicated that the FRP web diagonals played a key role in resisting the global bending stiffness of the unique structure, and thus, the shear deformation should be considered in the structural design in terms of stiffness-driven. When compared with the conventional calculation method for obtaining the bending stiffness of steel solid-web beams and planar trusses, the proposed method was more accurate and applicable for the unique hybrid structures.

Keywords: *hybrid structure, space truss, FRP, bending stiffness, equivalent continuum theory, homogenization-based model*

1. Introduction

Extrusion-type Fiber-Reinforced Polymer (FRP) profiles are particularly attractive for civil engineering applications owing to their unique advantages including a high strength-to-weight ratio and modular nature (Correia *et al.*, 2015; Gand *et al.*, 2013; Teng *et al.*, 2012). Currently, the use of extrusion-type FRP trusses is being gradually promoted for pedestrian and vehicular bridge constructions (Bai and Yang, 2013; Keller *et al.*, 2007; Kostopoulos, 2013; Morcous *et al.*, 2010; Sedlacek and Trumpf, 2004; Teixeira *et al.*, 2014). Trussed elements are mainly subjected to axial loading as opposed to shear loading, and so, they completely mobilize the axial mechanical characteristics of the unidirectional composite material. Concurrently, the inherent lack of material stiffness is compensated by the enhancement of the stiffness at the structural level. The loads are evenly distributed three-dimensionally, and thus, the inherent global structural bending stiffness significantly improves relative to that of solid web beams. Note that the flexural design of most of the aforementioned FRP trusses is stiffness-driven versus strength-driven owing to the relatively smaller elastic modulus compared to that of steel materials.

Recently, an innovative project was conducted to develop a new type of lightweight vehicular emergency bridge (Zhang *et al.*, 2014, 2016). The bridge enabled a unique FRP–aluminum spatial structure composed of two triangular deck–truss beams. As seen in Fig. 1, each of these triangular beams is characterized by an aluminum orthotropic deck supported by a series of interconnected extrusion-type FRP trussed elements located in the lower chords, web diagonals, and verticals. The orthotropic deck is welded onto other trussed members to form an integral structure and is considered as the upper chord. The FRP elements are connected by aluminum pieces with the aid of a pre-tightened teeth connection. As a new structure, it is noted that its detailed structural layout differs significantly from that of separated steel bridges in which the deck is detached from the trussed members (Durfee, 1986; Han *et al.*, 2015; Reis *et al.*, 2011). In previous studies, the structural performances of this bridge have been experimentally and numerically examined (Zhang *et al.*, 2014, 2016, 2018). The results indicated that such a unique structure

*Lecturer, College of Field Engineering, Army Engineering University of PLA, Nanjing 210007, China (Corresponding Author, E-mail: zhangdodo1986@sohu.com)
**Associate Professor, College of Field Engineering, Army Engineering University of PLA, Nanjing 210007, China (E-mail: 83812546@qq.com)
***Associate Professor, College of Field Engineering, Army Engineering University of PLA, Nanjing 210007, China (E-mail: shaofei@seu.edu.cn)
****Researcher, The Fourth Engineering Scientific Research Institute of PLA, Beijing 100850, China (E-mail: 598789085@qq.com)

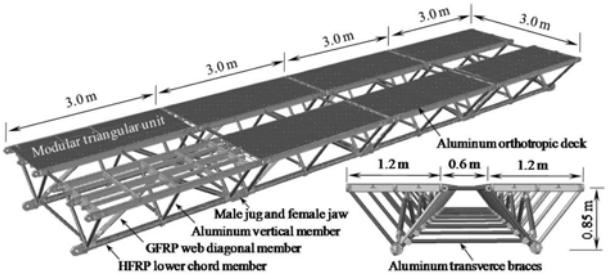

Fig. 1. Hybrid FRP–aluminum Spatial Deck–truss Structure and Its Modular Units

was also stiffness-driven as opposed to strength-driven. Thus, as a fundamental problem of theory of elasticity, which frequently occurs in engineering fields, bending stiffness is a key design index that affects normal use of the hybrid bridge, given the serviceability requirements.

Note that the bending stiffness of simple planar trusses is basically calculated using classical structural mechanics (Bao and Gong, 2006). However, for space trusses having intricate and hybrid configurations, the design and calculations are complex and time-consuming if the conventional method of structural mechanics is used, and thus, numerical simulation is performed as the primary method (Bai and Yang, 2013; Giannopoulos *et al*., 2003; Ju *et al*., 2011; Kostopoulos, 2013). Concurrently, during the preliminary design phase, modeling using a discrete finite element model can become computationally expensive. Therefore, it is inconvenient for engineers compared with employing a simplified theoretical method such as the explicit expressions, known from textbooks, for the bending stiffness of a simple solid-web beam. Consequently, simplified theoretical models have to be developed. However, there is a paucity of extant studies on simplified theoretical methods for the analysis of the large-scale FRP space trusses. In a previous study, a theoretical solution was developed to predict the deflection of a proposed hybrid deck–truss structure based on classical structural mechanics (Li *et al*., 2015). However, the derivation procedures and formulae in the analytical solution were relatively complex for a design-oriented application.

Therefore, a simpler theoretical solution for evaluating the equivalent bending stiffness of the unique hybrid deck–truss structure is desirable during the preliminary design phase. In this study, a simplified theoretical method was proposed to predict the equivalent bending stiffness of the above-mentioned structure. Based on previous experimental studies on the flexural behavior, a few reasonable assumptions were made for the derivation procedures, and the unique spatial deck–truss structure was first simplified as a planar truss model. Subsequently, the simplified planar truss model was transformed into a continuum solid-web beam using the equivalent continuum beam method. The formulae to predict the equivalent bending stiffness were then derived in a direct format using a simple calculation process. Finally, the theoretical predictions were compared with previously published experimental and numerical results.

2. Theoretical Methods

2.1 Equivalent Continuum Theory

With the advent of structural analysis programs using computers and increasing complexity of the numerical models for modern structures, equivalent continuum methods are beginning to be used by transforming an intricate structure (with discrete elements) into a simple equivalent continuum model, such as a shell, plate, and beam, based on the homogenization concept. Compared with the complex finite element model that requires a program with a high node and member capacity, an equivalent continuum method is beneficial in many ways: the number of degrees of freedom is reduced, input of the geometric parameter is much simpler, explicit expressions for the responses are known from textbooks (for simple structures like plates or beams), and structural behavior can be understood more easily (Noor, 1978). These advantages are valid particularly during the preliminary design phase where the determination of the global dimensions has priority over the concern of the structural details.

Equivalent continuum methods have proved to be a promising and practical solution for use in calculating the equivalent mechanical properties of cellular and lattice structures, particularly their effective stiffness, specific strength, plastic yield surface, and dynamic response (Abbes and Guo, 2010; Burgardt and Cartraud, 1999; Fan and Yang, 2006; Huybrechts and Tsai, 1996; Li *et al*., 2011; Mccallen and Romastad, 1988; Noor, 1988; Sun *et al*., 2013; Usik, 1994). The equivalence can be defined based on the energies, constitutive relations, or shearing equivalence principle, by transforming the load–displacement relationships of the cellular and lattice structures into the constitutive equations of the continuum model, such as a solid shell, monocoque, and beam (Burgardt and Cartraud, 1999). The key to continuum modeling is the determination of appropriate relationships of the material and geometric properties between the intricate structures and equivalent continuum model. Because of the numerous structural concepts, continuum modeling itself may not be unique.

To the best of knowledge of the authors, studies on the above-mentioned equivalent continuum methods for the analysis of the structural behavior of metal and FRP large-scale space truss structures are limited in the literature. A method was proposed aiming at the structural analysis of prestressed box–truss girders with concrete flanges and steel truss webs. In the method, the structure was converted into a thin-walled box girder through use of the shearing equivalence principle, and accordingly, the computing formulae for the element stiffness matrix were given (Komatsu and Nishimura, 1975; Wang *et al*., 2014). A theoretical method was employed to deduce the equivalent torsional stiffness of an all-composite triangular truss by considering it to be equivalent to a closed thin-walled beam based on the principle of equal single-cell shear stiffness (Xiong *et al*., 2015). However, it should be noted that the overall and detailed structural layouts of concrete-steel box–truss girders and composite triangular truss differ significantly from those of the proposed FRP–aluminum deck–truss structure. Concurrently, the existing theoretical models

were mainly derived for obtaining the torsional stiffness of the structures, rather than the bending stiffness. Therefore, the published theoretical models cannot be directly applied to the proposed hybrid deck–truss structure.

The present work is aimed to extend the equivalent continuum concept to the unique hybrid spatial deck–truss structure, particularly focusing on the structural spatial analysis problem of the global bending stiffness of the structure. In the theoretical derivation, the hybrid spatial deck–truss structure is transformed into a solid-web beam based on the homogenization concept and shearing equivalence principle. Subsequently, the computing formulae applicable to the global bending stiffness of the unique structure are derived. The advantage of using the equivalent beam method for the analysis of the hybrid spatial deck–truss structure is that the computer model is simplified by reducing the number of nodes and elements required in the calculation process. The equivalent procedure and derivation process are presented in the following section.

2.2 Derivation Procedure

In the equivalence procedure, first, the proposed spatial deck–truss structure is simplified as a planar truss model (see Fig. 2), which is similar to the approach in a previous study (Li *et al*., 2015). All the longitudinal I-type profiles and thin slab of the aluminum orthotropic deck are simplified as the upper chord where the used material, cross-sectional area, and axial stiffness of the former are identical to those of the latter. The original two vertical members are transformed into a single vertical member

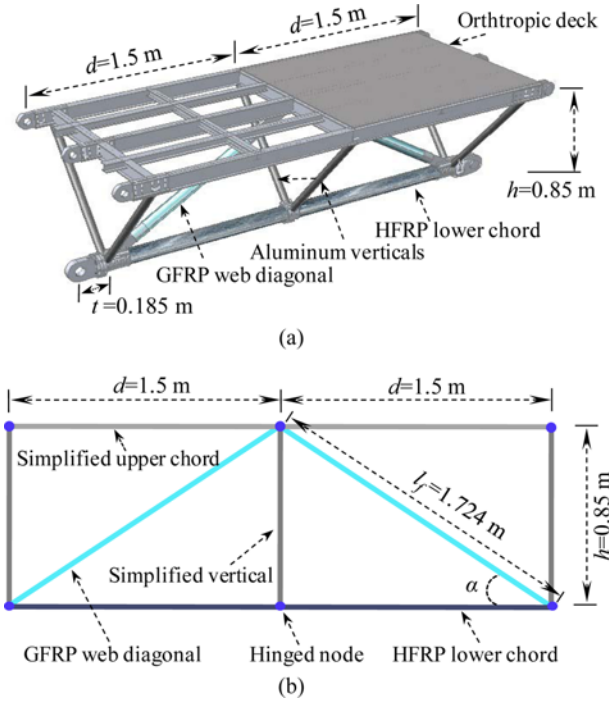

Fig. 2. Simplification of the Hybrid Spatial Deck–truss Structure into a Planar Truss Model: (a) Original Spatial Structure, (b) Simplified Planar Truss Model

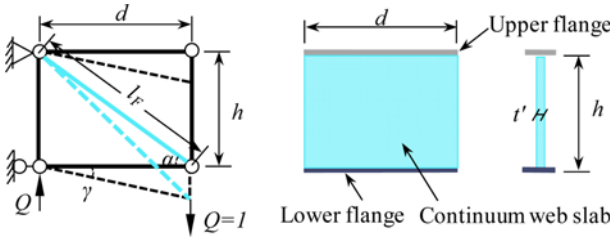

Fig. 3. Schematics of the Shear Deformation of a Segment of the Planar Truss subjected to a Unit Shear Load

of the simplified planar truss having the same cross-sectional area and axial tension–compression stiffness. Similarly, the original FRP lower chord and web diagonal are simplified to constitute the lower chord and web diagonal elements, respectively, in the simplified planar model. Furthermore, given the short distance, "*t*", between the pin-joint center and vertical member, the centers of the pin-joint and vertical member are assumed to be coincident. Given that the ratio of the sectional depth of the trussed elements to their length ratio is less than 1/10 and that an extremely small secondary stress is caused by the nodes (Bao and Gong, 2006), all the nodes are assumed as completely frictionless hinges.

By employing the simplified planar-truss model, the equivalent continuum process is subsequently characterized as a two-step process as follows: (1) The FRP web diagonals are transformed into a continuum solid-web slab based on the shearing equivalence principle (see Fig. 3). Note that in the continuum process, the equivalent web slab is only subject to shear loading; (2) by applying the homogenization concept, the equivalent upper and lower chords either remain unchanged or are transformed to the upper and lower flanges, respectively, of a continuum solid-web beam with a constant I-type cross-sectional area. It is assumed that the upper and lower flanges contribute to the same axial stiffness and sectional inertia-moment as the corresponding chord members. Finally, the bending stiffness of the equivalent continuum solid-web beam is derived using the classical beam theory (Bao and Gong, 2006). Next, the complete equivalence and homogenization procedure is introduced.

Figure 3 shows the deformation diagram of a segment of the planar truss that is subject to a unit shear load, $Q = 1$. Based on the load-transfer mechanism of an ideal planar truss, shear deformation γ of the segment is mainly caused by the axial deformation of the web diagonals. In this case, γ is expressed as follows:

$$\gamma \approx \tan\gamma = \frac{\delta_{11}}{d} = \frac{1}{d}\frac{N_F^2 l_F}{E_F A_F} \tag{1}$$

where δ_{11} denotes the flexibility coefficient of a segment subjected to a unit shear load, d denotes the length of a segment, and E_F, A_F, l_F, and N_F denote the elasticity modulus, cross-sectional area, effective length, and axial loads, respectively, of the GFRP (Glass Fiber-Reinforced Polymer) web diagonals. Based on the geometrical relationship, N_F, l_F, and d are given as follows:

$$N_F = \frac{1}{\sin\alpha},\ l_F = \frac{h}{\sin\alpha},\ d = h \cdot ctg\alpha \tag{2}$$

where α denotes the angle between the lower chord and web diagonal.

When Eq. (2) is substituted into Eq. (1) and rearranged, shear stiffness K of the simplified planar truss is obtained by Eq. (3). Shear stiffness K is contributed by the GFRP web diagonals and corresponds to the inverse of γ (i.e., $1/\gamma$). It should be noted that with respect to shear stiffness K, the contribution of the verticals is considered as low, and thus, is neglected in the derivation.

$$K = \frac{1}{\gamma} = E_F A_F \frac{dh^2}{l_F^3} \tag{3}$$

Thereafter, in the homogenization procedure, the web diagonals of the simplified planar truss model are transformed into a continuum solid-web slab, and this exhibits as an equal shear stiffness, K. It is assumed that the continuum solid-web slab has same length d, width h, and thickness t'. Its shear stiffness K is then given as follows:

$$K = G_F h t' \tag{4}$$

where G_F denotes the material shear modulus of the GFRP web slab.

When Eqs. (3) and (4) are incorporated and rearranged, the thickness t' of the equivalent solid-web slab is expressed as follows:

$$t' = \frac{E_F}{G_F} \cdot \frac{dh}{l_F^3} A_F \tag{5}$$

Based on the solid-web slab, the simplified planar truss model is further transformed into a solid-web beam with a constant I-type cross-sectional area. The upper and lower chords of the planar truss are transformed into the upper and lower flanges of the I-type solid-web beam, respectively. We assume that the equivalent upper and lower flanges with a flat rectangular cross-section enable an identical sectional inertia-moment (and axial stiffness) compared to the upper and lower chords, respectively. In this case, total linear-elastic deflection f of the equivalent solid-web beam that is induced by bending moment M and shear load Q is obtained based on the classical beam theory (Bao and Gong, 2006) as follows:

$$f = f_M + f_Q \tag{6}$$

where f_M and f_Q are given as follows:

$$\frac{d^2 f_M}{dx^2} = -\frac{M}{B_0} \tag{7}$$

$$\frac{df_Q}{dx} = \mu \cdot \frac{Q}{K} = \frac{\mu}{K} \cdot \frac{dM}{dx} \tag{8}$$

where B_0 denotes the bending stiffness of the solid-web beam, which is owing to the axial loading effect of the equivalent upper and lower flanges that resist bending moment M. K denotes the aforementioned shear stiffness of the equivalent web slab, and μ denotes the shear factor that is related to the characteristics of the cross-section of the equivalent web slab. With respect to a rectangular cross-section, $\mu = 1.2$.

Note that Eq. (7) is the usual calculation method without considering the shear deformation of the equivalent GFRP web slab. This equation is typically used in the conventional steel planar truss in which a small shear effect is observed in the calculation of the structural deformation (Bao and Gong, 2006). In Eq. (7), bending stiffness B_0 is given as follows:

$$B_0 = E_{x1}(I_{x1} + A_{x1}h_1^2) + E_{x2}(I_{x2} + A_{x2}h_2^2) \tag{9}$$

where E_{x1} and E_{x2} denote the material elastic modulus of the aluminum upper flanges and FRP lower flanges, respectively, I_{x1} and I_{x2} denote the sectional inertia-moment of the equivalent upper and lower flanges, respectively, and A_{x1} and A_{x2} denote the cross-sectional areas of the upper and lower flanges, respectively. Specifically, A_{x1} corresponds to the sum of the areas of the longitudinal I-type profiles and thin plate of the aluminum orthotropic deck, A_{x2} corresponds to that of the FRP lower chords, and h_1 (or h_2) denotes the distance from the centroidal axis of the upper flange (or the centroidal axis of the lower flange) to that of the equivalent web slab.

When rearranged, Eq. (6) is re-expressed as follows:

$$f = \frac{1}{\xi} f_M \tag{10}$$

and

$$\xi = \frac{1}{1 + \frac{f_Q}{f_M}} \tag{11}$$

where ξ denotes a coefficient that represents the effect of the shear deformation (induced by the equivalent web slab, i.e., the GFRP web diagonals) on the total linear-elastic deformation. Thus, ξ is termed as the shear influence coefficient.

It should be noted that with respect to the usual solid-web beams made of steel material, the contribution of the shear deformation to the total deflection of the beam is small, and thus, their shear influence coefficient ξ is almost equal to 1.0 (Bao and Gong, 2006). However, with respect to the presented unique hybrid structure, significant attention should focus on coefficient ξ. This is mainly because the pultruded GFRP materials exhibit an inherent lack of material stiffness and low elastic modulus.

Coefficient ξ is calculated by Eqs. (7), (8), and (10). This indicates that under the generic constraint and loading condition, ξ is a function of x. However, in the actual situation, ξ is almost equal to a constant. Coefficient ξ under three representative constraints and the loading situations is given as follows.

With respect to a simply supported beam subjected to a concentrated load at mid-span, ξ is calculated as follows:

$$\xi = \frac{1}{1 + \frac{f_Q}{f_M}} = \frac{1}{1 + \frac{12\mu B_0}{Kl^2}} \tag{12}$$

where l denotes the span length of the beam.

With respect to a cantilever beam with complete constraints at the fixed end and subjected to a concentrated load at the free end, ξ is obtained as follows:

$$\xi = \frac{1}{1+\frac{f_Q}{f_M}} = \frac{1}{1+\frac{3\mu B_0}{Kl^2}} \tag{13}$$

With respect to a simply supported beam that is subject to a four-point bending load, ζ is given as follows:

$$\zeta = \frac{1}{1+\frac{f_Q}{f_M}} = \frac{1}{1+\frac{3\mu B_0}{20Kd^2}} \tag{14}$$

Given that ξ corresponds to or is less than 1.0 ($\xi \leq 1$), it is, therefore, viewed as reduction factor of the shear effect of the web slab to bending stiffness B_0. Thus, total bending stiffness B of the equivalent continuum solid web beam by considering the shear effect of the GFRP web slab is given as follows:

$$B = \xi B_0 \tag{15}$$

where B_0 is calculated by Eq. (9).

Finally, based on equivalent bending stiffness B, the differential equation of the total linear-elastic deflection is obtained as follows:

$$\frac{d^2 f}{dx^2} = \frac{M}{B} \tag{16}$$

2.3 Discussions

As demonstrated in the above-mentioned theoretical method, the simplified theoretical model was derived using an equivalent continuum method based on the homogenization concept and shearing equivalence principle. The unique hybrid spatial deck–truss structure was finally transformed into a single solid-web beam with a constant cross-sectional area. The present derivation procedure of such an equivalent continuum model was relatively simple, and a total of 16 equations were employed.

Note that in a previously published study (Li *et al.*, 2015), a theoretical model was also derived for calculating the deflection of the unique hybrid deck–truss structure. However, the theoretical model was derived via the Mohr formulas (known from textbooks), and the corresponding formulation conversion was determined according to classical structural mechanics (Bao and Gong, 2006). In the derivation procedure, the unique hybrid deck–truss structure was finally transformed into two solid-web beams, which were different from the single solid-web beam presented in this paper. Concurrently, the derivation procedure in the previous theoretical method was complex, and a total of 39 equations were employed.

In general, compared to the previously published theoretical method (Li *et al.*, 2015), the simplified theoretical model in the present paper features a more simple and explicit expression for the equivalent bending stiffness of the unique structure, which can be understood more easily. From this perspective, compared to the published theoretical method, the proposed simplified theoretical method exhibits a remarkable advantage. Moreover, during the derivation process, the shear deformation of the equivalent GFRP web slab was considered in the calculation of the total deflection of the continuum solid beam, which is much different from the usual calculation method for calculating the conventional steel planar truss.

3. Verification

3.1 Experimental Procedure

In previous studies (Zhang, 2016; Zhang *et al.*, 2014), two bridge prototypes having the same structural form of the unique hybrid deck–truss structures have been designed and fabricated. Among them, one was designed with a length of 12 m, width of 1.2 m, and depth of 0.85 m, whereas the other was designed with a length of 24 m, width of 1.2 m, and depth of 1.2 m. Full-scale bending loading tests and numerical simulations were performed to evaluate the actual linearly elastic flexural behavior. In the present technical study, the theoretical predictions will be validated by the previously published experimental and numerical results of a 12-m-bridge model (Zhang *et al.*, 2014). Owing to the space limitations and for avoiding repetition, the detailed verification procedure of the simplified theoretical model by the new 24-m-prototype bridge is not reiterated herein because it demonstrates similar regular patterns and findings. The experimental procedure and numerical model performed on the 12-m-bridge model are briefly described as follows.

In the experiments, four pre-fabricated triangular units were mounted as a 12 m simply supported full-scale experimental structure and subjected to a four-point bending loading test. As displayed in Fig. 4, the load configuration is symmetric. The distance between the two loading areas is 3.0 m. The loads are applied vertically by the hydraulic jack that is attached to the compression transbeam of the counterforce frame. The applied loads are then transferred to the two loading areas on the top surface of the bridge deck by the spreader beam. To measure the applied loads, a load cell is positioned between the hydraulic jack and compression transbeam. Two loading steps were applied. In the first step, a load from 0 kN to 56 kN was applied at an

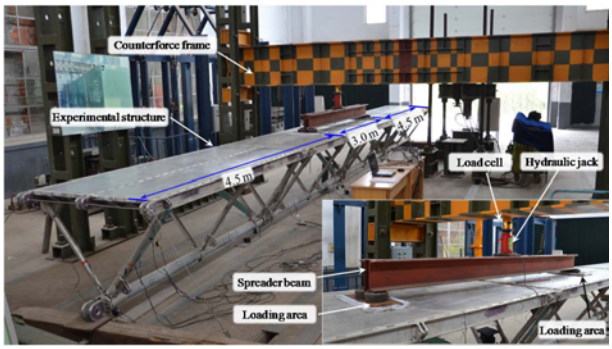

Fig. 4. Experimental Set-up of the Static Four-point Bending Load Test

interval of 4.0 kN, whereas in the second step, a load from 56 kN to 75 kN was applied at an interval of 2.0 kN. The vertical displacement of the structure was recorded using an electronic displacement meter. The experiments indicated that the load–displacement response curve varied practically linearly, with no residual displacement after loading, so that the bridge model was near the linear-elastic range under the serviceability limit state.

3.2 Numerical Model

A three-dimensional finite element model was constructed using ANSYS 12.0 (see Fig. 5) (Zhang *et al.*, 2014; Li *et al.*, 2015). To accurately simulate the proposed triangular deck–truss structure and its various structural members, two types of elements (shell and beam elements) were employed. Shell-63 element with a linear shape function was used to simulate the aluminum thin slab, and a mesh size of 100 mm was employed. Beam-188 element with tension–compression and bending capabilities was employed to simulate the crisscrossing aluminum I-type profiles, and a mesh size of 100 mm was selected. Beam-188 element was also used to model the GFRP trussed elements that mainly endure internal axial forces, and the number of element divisions was set as 10. The connectors were simplified as a segment of their conterminous chord members, and the number of element divisions was set as 10. All the joints between the trussed elements defaulted to rigid nodes. The total number of elements was 3506 and 5952 for the Beam-188 and Shell-63 elements, respectively.

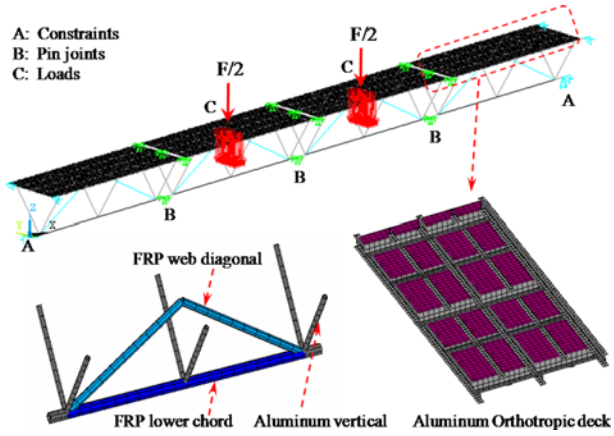

Fig. 5. Schematics of the Three-dimensional Numerical Model

Table 1. Mechanical Properties of the Used Materials

Material type	Modulus of elasticity (GPa)	Poisson's ratio
HFRP	E_l = 61.6*	v_{12} = 0.31
GFRP	E_l = 31.5*	v_{12} = 0.28
Al alloy	E = 68.5	v = 0.33

*E_l denotes the elastic modulus in the longitudinal direction of the extrusion-type FRP tubes.

In the finite element model, the generalized Hooke's law for linear-elastic isotropic materials was used as the constitutive material law for the aluminum profiles. The generalized Hooke's law for linear-elastic anisotropic materials was also applied to the extrusion-type FRP elements owing to its unidirectional characteristic. The mechanical properties that were used as inputs are listed in Table 1. The nonlinear behavior of the materials was not considered for the linear-elastic model. The buckling issue of the compressive members and dead weight of the structure were also not considered because the experimental strain was within the linear strain range. The displacement boundary and loading conditions were performed in accordance with the experimental procedure. More information about the finite element model is available in previous works (Zhang *et al.*, 2014; Li *et al.*, 2015).

3.3 Comparisons and Discussions

In the theoretical calculation, the multi-parameters used in the simplified equivalent continuum model are listed in Table 2. Based on the parameters, shear stiffness K contributed by the GFRP web diagonals was calculated using Eq. (3) and bending stiffness B_0 without considering the shear deformation of the equivalent GFRP web slab was obtained using Eq. (9). When the values of K and B_0 were substituted into Eq. (14), coefficient ξ (under a four-point loading condition corresponding to the experiments) was obtained as 0.574. Thereafter, total bending stiffness B of the equivalent continuum solid-web beam was calculated using Eq. (15). Finally, the deflection at the mid-span of the equivalent continuum solid-web beam was obtained using the derived formula in Eq. (16). Note that in the theoretical calculation, the constraint condition of the theoretical model was same as that for the static four-point bending loading test. Because the experimental load–displacement response curve of the prototype bridge varied almost linearly with no residual

Table 2. Parameters used in the Simplified Equivalent Continuum Theoretical Model

Trussed elements	Cross-sectional area	Effective length	Elastic moduli	Sectional inertia-moment	Centroidal distance
Upper chords	A_{x1} = 9440 mm^2	l_{x1} = 1500 mm	E_{x1} = 68.5 GPa	I_{x1} = 4026158 mm^4	h_1 = 159 mm
Lower chords	A_{x2} = 2411 mm^2	l_{x2} = 1500 mm	E_{x2} = 61.6 GPa	I_{x2} = 2790000 mm^4	h_2 = 691 mm
Web diagonals	A_F = 1418 mm^2	L_F = 1724 mm	E_F = 31.5 GPa	---	---
Web verticals	A_Z = 1775 mm^2	L_Z = 850 mm	E_1 = 68.5 GPa	---	---

Other parameters used in the theoretical model:

Length of structure:	L = 12 m	Height of model:	h = 0.85 m	Length of one unit:	d = 1.5 m
Shear factor:	μ = 1.2	Shear stiffness :	K = 9.45 × 10^6 MPa·mm^2	Bending stiffness:	B_0 = 8.77 × 10^7 N·m^2

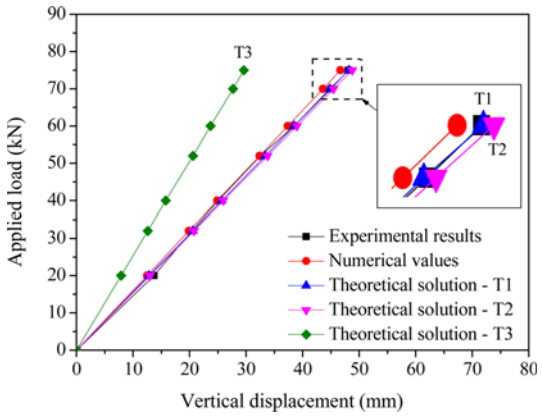

Fig. 6. Theoretical Solutions of the Load–displacement Curve and Their Comparison with the Experimental Results and Numerical Simulations

displacement under the design loading level of 75 kN, only seven loading levels, corresponding to 20, 32, 40, 52, 60, 70, and 75 kN, were selected from the experimental two loading steps, and then compared with the theoretical curves.

Figure 6 shows the theoretical load–displacement curve obtained from Eq. (16) (denoted by "T1") and its comparison with the experimental results and numerical predictions. Additionally, the theoretical solution obtained from a previously published study (Li *et al*., 2015) is plotted (denoted by "T2"). Concurrently, the theoretical solution calculated from Eq. (7) is presented (denoted by "T3"). As indicated earlier in the theoretical derivation process, Eq. (7) is the usual calculation method without considering the shear deformation of the equivalent web slab for the total deflection of the continuum solid beam. However, in theoretical solutions T1 and T2, the shear deformation of the equivalent GFRP web slab was considered in the total deflection of the equivalent continuum model. It is observed that all the three theoretical curves (T1, T2, and T3) exhibit a linear variation under the serviceability limit state loading level. This is identical to that of the experimental and numerical curves.

As clearly observed in Fig. 6, the theoretical solution T3 exhibits a large discrepancy from the experimental results and numerical predictions. The maximum difference between T3 and the experimental results is approximately 38.5%. This finding indicates that the usual calculation method of Eq. (7) is not suitable for calculating the bending stiffness of the proposed unique hybrid FRP–aluminum deck–truss structure. This is mainly because the shear deformation of the GFRP web diagonals was not considered in the total elastic deflection of the structure. Therefore, the shear deformation of the GFRP web diagonals contribute significantly to the total elastic deflection of the structure, and thus, cannot be neglected. This result is considerably different from that of the conventional steel planar truss where a small shear effect is observed in the calculation of the structural deformation, and thus, is typically neglected in the usual calculation method (Bao and Gong, 2006).

Compared with theoretical solution T3, however, theoretical solution T1 correlates well with the experimental results and numerical predictions, which proves the validity of the simplified theoretical model proposed in the paper. The difference between T1 and the experimental results and numerical predictions is extremely small. For example, at a design loading level of 75 kN, the maximum difference between T1 and the experimental results is approximately 0.2%, whereas the corresponding maximum difference between T1 and the numerical predictions is approximately 3.2%. Thus, the proposed simplified equivalent continuum method and its computing model can be used to predict the flexural deformation for the unique structure with a satisfactory accuracy. This is mainly because the shear deformation of the equivalent GFRP web slab was taken into account in the calculation of the total deflection of the equivalent continuum solid-web beam. Compared with the usual calculation method, T3, proposed simplified theoretical method T1 exhibits a remarkable precision.

Furthermore, Fig. 6 demonstrates that theoretical solutions T1 and T2 correlate well with each other with a maximum difference of approximately 1.2%. Both theoretical solutions T1 and T2 are larger than the experimental results, indicating that the theoretical model over-predicts the actual vertical deformation. Moreover, it is demonstrated that theoretical solution T1 provides a higher accuracy than T2. For example, at the design loading level of 75 kN, the maximum difference between T1 and the experimental results is approximately 0.2%, whereas the corresponding maximum difference between T2 and the numerical simulation is approximately 1.5%. This is mainly because, as indicated by a previous theoretical study (Li *et al*., 2015), the deflection contributed by the shear deformation of the vertical members is extremely small, which is calculated in theoretical solution T2 but is not considered in theoretical solution T1.

Using Eqs. (3), (9), and (14), the global bending stiffness of the theoretical solution T1 is obtained as 5.16×10^7 N·m. According to the previously published results (Zhang *et al.*, 2014), the experimental and numerical bending stiffness as obtained by linear fitting of the corresponding load–displacement curves are 5.09 ×1 0^7 N·m^2 and 5.45×10^7 N·m^2, respectively. Thus, the theoretical predictions provides larger magnitudes of the bending stiffness with a difference of < 1.4% when relative to the experiments and < 5.3% relative to the numerical simulation. Generally, the proposed equivalent continuum model in terms of a solid-web beam and derived via the homogenization concept and shearing equivalence principle, is proved to be a promising and practical solution for calculating the global bending stiffness of the unique hybrid FRP–aluminum deck–truss structure.

It is considered that the difference between theoretical solution T1 and experimental results was mainly owing to the dissimilarities in the nodal stiffness, local structural configuration, and aforementioned *t* value. For example, the actual nodal joints of the experimental structure were not well modeled in the analytical model in the derivation process of the equivalent continuum theoretical model. The nodal stiffness of the theoretical model was larger than that of the real structure owing to the imperfectly

rigid joints, and thereby caused an over-prediction of the actual bending stiffness in the theoretical prediction. The difference between theoretical solution T1 and the numerical model may also be potentially attributed to the dissimilarities in the nodal stiffness. For example, a rigid-jointed node exists in the numerical model, whereas a hinged-jointed mode is presented in the theoretical solution; moreover, the detailed modeling of the nodal joints is different for the numerical and theoretical models.

4. Conclusions

The study presented a simplified theoretical solution for the evaluation of the equivalent bending stiffness of a unique hybrid FRP–aluminum spatial deck–truss structure. Based on the equivalent shearing principle and complete homogenization concept, an equivalent continuum beam method was proposed for the theoretical derivation, in which the spatial deck–truss structure was transformed into an equivalent solid-web beam with a constant cross-sectional area. The suggested formulae feature a direct format and simple calculation process that will be convenient for engineers in terms of the calculation and design purpose. The theoretical solutions were experimentally calibrated by previously published full-scale bending loading tests and numerical simulations. The strong correlations between the theoretical predictions, experimental results, and numerical simulations provided sufficient confidence in the validity of the suggested theoretical method for the unique structure. Compared with the published theoretical method, the proposed simplified theoretical method exhibited a remarkable advantage.

Furthermore, the results indicated that the shear deformation of the unique structure induced by the axial deformation of the GFRP web diagonals played a key role in resisting the global bending stiffness and hence, the focus should be on structural design for flexural deformation. In comparison, in the typical calculation method for the conventional steel solid web beams or planar trusses for which the shear deformation is sufficiently small. The suggested theoretical method was more applicable in terms of estimating the equivalent global bending stiffness for the unique hybrid FRP–aluminum spatial deck–truss structure. The proposed theoretical solutions could be applied in design applications and optimization and also be expected to constitute a valuable approach for promoting the development of lightweight structural systems. Furthermore, the presented computing model is potentially useful to be developed for analogous composite space truss structures.

Acknowledgements

Financial supports from National Key Research and Development Program of China (2017YFC0703008), Natural Science Foundations of Jiangsu Province (BK20170752), National Natural Science Foundation of China (51708552, 51778620, 51608524), and Young Elite Scientist Sponsorship are gratefully acknowledged.

References

Abbes, B. and Guo, Y. Q. (2010). "Analytical homogenization for torsion of orthotropic sandwich plates: Application to corrugated cardboard." *Composite Structures*, Vol. 92, No. 3, pp. 699-706, DOI: 10.1016/j.compstruct.2009.09.020.

Bai, Y. and Yang, X. (2013). "Novel joint for assembly of all-composite space truss structures: Conceptual design and preliminary study." *Journal of Composite for Construction*, Vol. 17, No. 1, pp. 130-138, DOI: 10.1061/(ASCE)CC.1943-5614.0000304.

Bao, S. H. and Gong, Y. G. (2006). *Structural mechanics*, Wuhan University of Technology Press, Wuhan, China.

Burgardt, B. and Cartraud, P. (1999). "Continuum modeling of beamlike lattice trusses using averaging methods." *Computers & Structures*, Vol. 73, No. 15, pp. 267-279, DOI: 10.1016/S0045-7949(98)00274-0.

Correia, J. R., Bai, Y., and Keller, T. (2015). "A review of the fire behavior of pultruded GFRP structural profiles for civil engineering applications." *Composite Structures*, Vol. 127, pp. 267-287, DOI: 10.1016/j.compstruct.2015.03.006.

Durfee, R. H. (1986). "Review of triangular cross section truss systems." *Journal of Structural Engineering*, Vol. 112, No. 5, pp. 1088-1096, DOI: 10.1061/(ASCE)0733-9445(1986)112:5(1088).

Fan, H. L. and Yang, W. (2006). "An equivalent continuum method of lattice structures." *Acta Mechanica Solida Sinica*, Vol. 19, No. 2, pp. 103-113, DOI: 10.1007/s10338-006-0612-x.

Gand, A. K., Chan, T. M., and Mottram, J. T. (2013). "Civil and structural engineering applications, recent trends, research and developments on pultruded fiber reinforced polymer closed sections: A review." *Frontiers of Structural & Civil Engineering*, Vol. 7, No. 3, pp. 227-244, DOI: 10.1007/s11709-013-0216-8.

Giannopoulos, G., Vantomme, J., Wastiels, J., and Taerwe, L. (2003). "Numerical analysis and experimental validation for static loads of a composite bridge structure." *Composite Structures*, Vol. 62, No. 2, pp. 235-243, DOI: 10.1016/S0263-8223(03)00118-1.

Han, L. H., Xu, W., He, S. H., and Tao, Z. (2015). "Flexural behavior of concrete filled steel tubular (SFST) chord to hollow tubular brace truss: Experiments." *Journal of Constructional Steel Research*, Vol. 109, pp. 137-151, DOI: 10.1016/j.jcsr.2015.03.002.

Huybrechts, S. and Tsai, S.W. (1996). "Analysis and behavior of grid structures." *Composite Science and Technology*, Vol. 56, No. 9, pp. 1001-1015, DOI: 10.1016/0266-3538(96)00063-2.

Ju, S., Jiang, D. Z., and Shenoi, R. A. (2011). "Flexural properties of lightweight FRP composite truss structures." *Journal of Composite Materials*, Vol. 45, No. 19, pp. 1921-1930, DOI: 10.1177/0021998311410237.

Keller, T., Bai, Y., and Vallée, T. (2007). "Long-term performance of a glass fiber-reinforced polymer truss bridge." *Journal of Composite for Construction*, Vol. 11, No. 1, pp. 99-108, DOI: 10.1061/(ASCE)1090-0268(2007)11:1(99).

Komatsu, S. and Nishimura, N. (1975). "Three dimensional analysis of truss girders by the thin walled elastic beam theory." *Journal of Structural Mechanics and Earthquake Engineering*, Vol. 1975, No. 236, pp. 15-29, DOI: 10.2208/jscej1969.1975.238_1.

Kostopoulos, V. (2013). "Design and construction of a vehicular bridge made of glass/polyester pultruded box beams." *Plastics, Rubber & Composites*, Vol. 34, No. 4, pp. 201-207, DOI: 10.1179/174328905X55641.

Li, M., Wu, L. Z., Ma, L., Xiong, J., and Guan, Z. X. (2011). "Torsion of carbon fiber composite pyramidal core sandwich plates." *Composite Structures*, Vol. 93, No. 9, pp. 2358-2367, DOI: 10.1016/j.compstruct.2011.03.024.

Li, F., Zhang, D. D., Zhao, Q. L., and Deng A. Z. (2015). "A simple analytical solution for predicting the deflection of a hybrid FRP-aluminum modular space truss bridge." *Journal of Central South University*, Vol. 22, No. 11, pp. 4414-4425, DOI: 10.1007/s11771-015-2989-5.

Mccallen, D. B. and Romastad, K. M. (1988). "A continuum model for the nonlinear analysis of beam-like lattice structures." *Computer & Structures*, Vol. 29, No. 2, pp. 177-197, DOI: 10.1016/0045-7949(88)90252-0.

Morcous, G., Cho, Y., El-Safty, A., and Chen, G. (2010). "Structural behavior of FRP sandwich panels for bridge decks." *KSCE Journal of Civil Engineering*, Vol. 14, No. 6, pp. 879-888, DOI: 10.1007/s12205-010-1025-4.

Noor, A. K. (1988). "Continuum models for repetitive lattice structures." *Applied Mechanics Reviews*, Vol. 41, No. 7, pp. 285-296, DOI: 10.1115/1.3151907.

Noor, A. K., Anderson, M. S., and Greene, W. H. (1978). "Continuum models for beam- and platelike lattice structures." *Aiaa Journal*, Vol. 16, No. 12, pp. 1219-1228, DOI: 10.1115/1.3151907.

Reis, A. and Pedro, J. J. O. (2011). "Composite truss bridges: New trends, design and research." *Steel Construction*, Vol. 4, No. 3, pp. 176-182, DOI: 10.1002/stco.201110024.

Sedlacek, G. and Trumpf, H. (2004). "Development of a lightweight emergency bridge." *Structural Engineering International*, Vol. 14, No. 4, pp. 282-287, DOI: 10.2749/101686604777963702.

Sun, F. F., Fan, H. L., Zhou, C. W., and Fang, D. N. (2013). "Equivalent analysis and failure prediction of quasi-isotropic composite sandwich cylinder with lattice core under uniaxial compression." *Composite Structures*, Vol. 101, pp. 180-190, DOI: 10.1016/j.compstruct.2013.02.005.

Teixeira, A. M. A. J., Pfeil, M. S., and Battista, R. C. (2014). "Structural evaluation of a GFRP truss girder for a deployable bridge." *Composite Structures*, Vol. 110, pp. 29-38, DOI: 10.1016/j.compstruct.2013.11.014.

Teng, J. G., Yu, T., and Fernando, D. (2012). "Strengthening of steel structures with fiber-reinforced polymer composites." *Journal of Constructional Steel Research*, Vol. 78, pp. 131-143, DOI: 10.1016/j.jcsr.2012.06.011.

Usik, L. (1994). "Equivalent continuum models of large plate-like lattice structures." *International Journal of Solids & Structures*, Vol. 31, No. 4, pp. 457-467, DOI: 10.1016/0020-7683(94)90086-8.

Wang, T., Xie, X., Wang, Y., and Shi, P. C. (2014). "Analysis of prestressed composite truss girders with steel truss webs." *Journal of Zhejiang University*, Vol. 48, No. 4, pp. 711-720, DOI: 10.3785/j.issn.1008-973X.2014.04.022.

Xiong, B., Luo, X. L., and Tan, H. F. (2015). "Analysis of torsional stiffness of all-composite truss." *Acta Materiae Composite Sinica*, Vol. 32, No. 2, pp. 501-507, DOI: 10.13801/j.cnki.fhclxb.20140627.003.

Zhang, D. D. (2016). *Load-carrying properties and calculation methods of a novel hybrid FRP-metal space truss bridge*, PhD Thesis, PLA Univ. of Sci. & Tech, Nanjing, China.

Zhang, D. D., Zhao, Q. L., Huang, Y. X., Li, F., Chen H. S., and Miao, D. S. (2014). "Flexural properties of a lightweight hybrid FRP-aluminum modular space truss bridge system." *Composite Structures*, Vol. 108, pp. 600-615, DOI: 10.1016/j.compstruct.2013.09.058.

Zhang, D. D., Zhao, Q. L., Li, F., Gao, Y. F., and Tao, J. (2018). "Torsional behavior of a hybrid FRP-aluminum space truss bridge: Experimental and numerical study." *Engineering Structures*, Vol. 157, pp. 132-143, DOI: 10.1016/j.engstruct.2017.12.013.

Zhang, D. D., Zhao, Q. L., Li, F., and Li, F. (2016). "Experimental and theoretical study of the torsional mechanism of a hybrid FRP-aluminum triangular deck-truss structure." *KSCE Journal of Civil Engineering*, Vol. 26, No. 6, pp. 2447-2456, DOI: 10.1007/s12205-015-0257-8.